Scaling Behavior and Self-Organization in Plasma Turbulence

P. Tham and A. K. Sen
Plasma Physics Laboratory, Columbia University, New York, New York 10027
(Received 12 August 1993)

The nonlinearly saturated fluctuation level scaling with linear growth rate is presented for two instabilities: the ion temperature gradient instability and the rotationally driven $\mathbf{E} \times \mathbf{B}$ instability. In some instances, the plasma self-organizes from plasma turbulence and evolves into a quasicoherent state. In the turbulent state, spectral broadening is observed. The emergence of the semicoherent state is reflected by a narrowing spectral width of the mode with higher linear growth rates and fluctuation levels. The fine structure in the spectral width is resolved and indicates the presence of radial harmonics. The increasing coherence is also supported by a bispectral analysis.

PACS numbers: 52.35.Mw, 52.25.Gj, 52.35.Ra

Developing an understanding of the nonlinearly saturated state of plasma instabilities is important because it is generally believed that microinstability-induced turbulent diffusion is responsible for the observed anomalous transport in plasmas [1–3]. Many nonlinear theories, from the simple mixing length estimates, resonance broadening theory [4,5], to the sophisticated renormalized theories [6], have been advanced to explain the broadband spectral characteristics of the turbulence. Recently considerable research has focused on plasma self-organization and the development of coherent structures like vortices and solitons [7–10]. The final nonlinearly saturated state may be composed of contributions from both turbulent and coherent structures coexisting in the plasma.

Experimentally in small machines like the Columbia Linear Machine (CLM), plasma instabilities are often observed in their nonlinearly saturated states as a single spectral feature with an associated spectral width above the broadband plasma turbulence. This width is the result of nonlinear processes. The spectral width may be an indication that the mode is composed of many radial harmonics, leading to the claim that the plasma is in a nonlinearly turbulent state through wave-wave interactions. Thus the spectral width and the linear growth rate of the instability are two parameters characterizing the strength of the turbulence indicated by the fluctuation level.

In this Letter, the scaling of the fluctuation level with linear growth rate for two plasma instabilities is presented. The results are characteristic of the two limits of weak and strong turbulence. For the ion temperature gradient (ITG) instability, a quadratic scaling of the linear growth rate with the fluctuation level is observed which is characteristic of the weak turbulence regime. The $\mathbf{E} \times \mathbf{B}$ instability shows two markedly different behaviors in the nonlinear saturated state of the plasma instability. In one case, the spectral width exhibited the broadening of the spectral width with increasing electrostatic fluctuation levels, expected in a strong turbulence regime. However, in the other case, the spectral width actually *narrowed* with increasing fluctuation level. Moreover, both regimes exhibited a linear scaling of linear growth rate with the electrostatic fluctuation level. We investigate the dependence of the spectral width on the fluctuation level and show experimentally that the plasma self-organizes from its turbulent state and evolves into a quasicoherent state. The quasicoherent state is also observed to be composed of radial harmonics, which is coupled to the turbulence justifying the link to turbulence and transport.

The experiments were conducted in the CLM where the plasma is produced by a hot cathode dc discharge. Typical plasma parameters in the experimental cell were density 1×10^9 cm^{-3}, electron temperature ~ 8 eV, parallel ion temperature $\sim$ 5–18 eV, perpendicular ion temperature ~ 8 eV, magnetic field 1 kG, and plasma column radius ~ 3.0 cm. The slab branch of the ITG mode was produced via the rf heating technique [11]. The $\mathbf{E} \times \mathbf{B}$ mode, which is always present in our machine, is a Rayleigh-Taylor type flute mode driven unstable by the $\mathbf{E} \times \mathbf{B}$ rotation of the plasma column. The growth rates for these two modes were measured via gated feedback [12].

The dependence of the saturated mode amplitude with the linear growth rate of the ITG mode is displayed in Fig. 1. The linear growth rate γ of the ITG instability is normalized to the real frequency of the ITG mode ω_r.

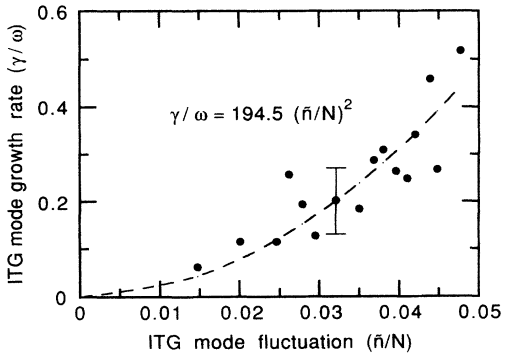

FIG. 1. Normalized linear growth rate vs fluctuation levels for the ITG instability.

0031-9007/94/72(7)/1020(4)$06.00

The saturated amplitude level $\tilde{n}_{sat}$ was determined by taking the square root of the power spectrum integrated about the mode frequency with a bandwidth of $\sim$ 40 kHz. The saturated amplitude $\tilde{n}_{sat}$ is normalized to the plasma density n_0. The saturated amplitude of the ITG mode was varied by changing the endplate bias and the rf heating voltage. A linear regression fit to the data with a power law scaling model of the form

$$\frac{\gamma}{\omega} \propto \left(\frac{\tilde{n}_{sat}}{n_0}\right)^{\alpha} \quad (1)$$

was performed to obtain the experimental scaling relationship. The dashed line in Fig. 1 shows a quadratic fit of the linear growth rate with the nonlinear saturated fluctuation level. The fit is reasonably good and so this quadratic scaling suggests a weak turbulent regime for these ranges of fluctuation levels. Such a quadratic scaling between the linear growth rate and the fluctuation levels has been previously obtained for many plasma instabilities [12–14] in the weak turbulence limit.

The $\mathbf{E}\times\mathbf{B}$ fluctuation amplitude was modified by ranging only the endplate bias from 0 to 10 V. The scaling for the $\mathbf{E}\times\mathbf{B}$ rotationally driven flute mode is shown in Fig. 2(a). The linear growth rate was normalized to the $\mathbf{E}\times\mathbf{B}$ rotation frequency in the laboratory frame. It was discovered that the data points clustered into two groups which we labeled (i) and (ii). Group (i) corresponds to a weak, low amplitude $\mathbf{E}\times\mathbf{B}$ mode while group (ii) corresponds to a strong, high amplitude mode. It will be shown below that (i) corresponds to a turbulent regime and (ii) corresponds to a quasicoherent regime. Both groups show that the saturated mode amplitude depends linearly on the linear growth rate, in contrast to the quadratic scaling obtained for the ITG instability. This linear relationship between the linear growth rate and the saturated amplitude is consistent with a strong turbulence type scaling [15].

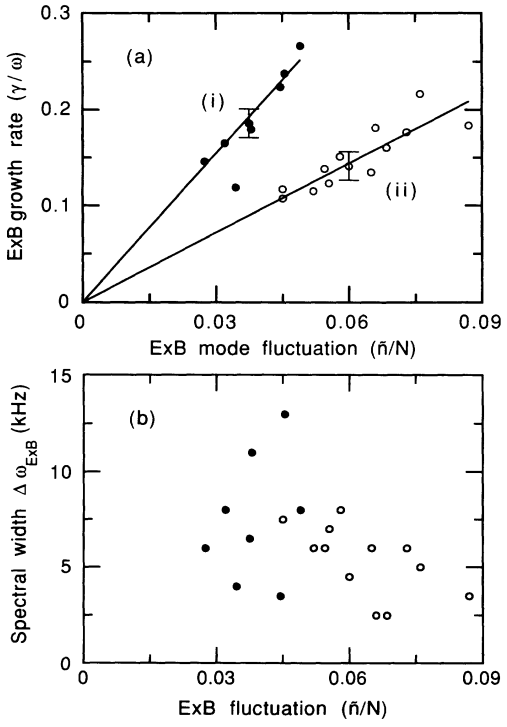

FIG. 2. Scaling for the $\mathbf{E}\times\mathbf{B}$ mode. (a) Normalized linear growth rate vs fluctuation levels; (b) variation of spectral width with saturated amplitude.

The two different linear scalings are characterized by different behavior of the spectral width as a function of increasing fluctuation level. The spectral widths for the data shown in Fig. 2(a) are plotted in Fig. 2(b) where the spectral width is taken to be the full width at half maximum (FWHM) of the mode spectrum. Two general trends are observed, even though there is a fairly large scatter among the data points. The solid dots [corresponding to case (i) of Fig. 2(a)] correspond to a more turbulent nonlinear state. The spectral width is broadened as expected as the mode gets stronger [16]. The open circles [corresponding to case (ii) of Fig. 2(a)] correspond to a coherent mode behavior. In this case, the spectral width gets narrower as the mode gets stronger. We attribute this phenomenon to an evolution into a quasicoherent state. It is interesting to note that the experimental scaling relationship of the growth rate with the saturated amplitude for both the coherent state and turbulence exhibited a linear scaling.

A bispectral analysis was conducted to investigate further this coherent regime. The autobispectrum [17] was used to determine the level of coherence of various frequency components in the spectrum based on three-wave nonlinear interactions. The autobispectrum is a one point measurement and a single Langmuir probe was used to accumulate the time series data under various conditions at various radial and axial positions. The normalized autobispectrum, called the autobicoherency, is defined as

$$b^2(\omega_1,\omega_2) = \frac{|E(X_{\omega_1}X_{\omega_2}X_{\omega_1+\omega_2})|^2}{E(|X_{\omega_1}X_{\omega_2}|^2)E(|X_{\omega_1+\omega_2}|^2)}, \quad (2)$$

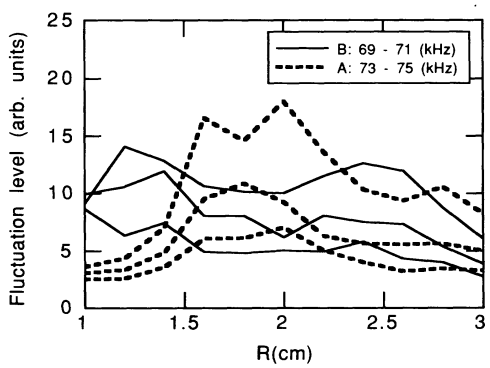

FIG. 3. Mode structure of the radial harmonics for the $\mathbf{E}\times\mathbf{B}$ mode.

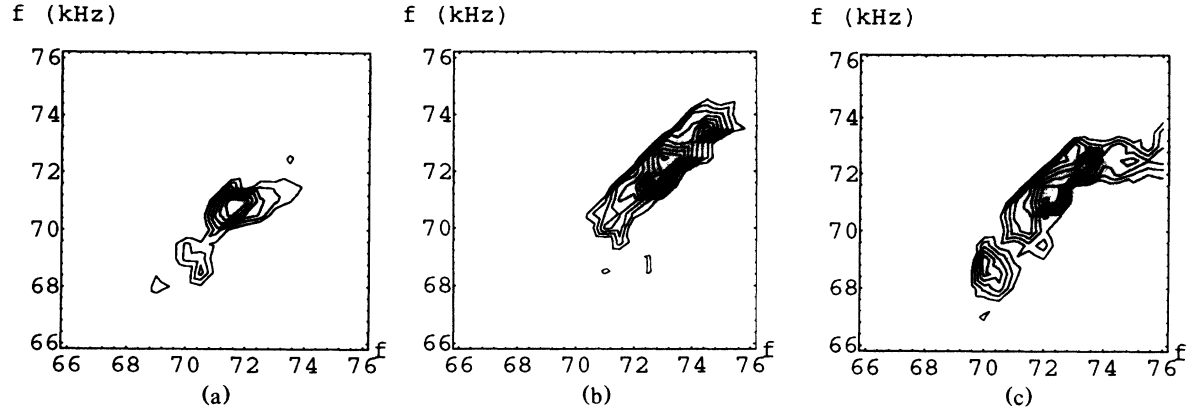

FIG. 4. Contour plots of autobicoherency (0.1–0.5) at different radii (a) 1.2 cm, (b) 1.8 cm, and (c) 2.4 cm.

with the range of values limited to $0 \leq b^2(\omega_1, \omega_2) \leq 1$. The X's are the Fourier amplitudes of the time series data and E is the expectation value. The number of data points N determines the frequency resolution Δf which is given by $\Delta f = 1/T$ with $T = N\Delta t$ and Δt the sampling interval. For these measurements, the frequency resolution was ~ 8 kHz while the statistical uncertainty was ≤ 0.01 ($\sim 1/M$, where M is the number of realizations). Since CLM is a steady-state machine, many time series were accumulated by repeated measurements and stored. It was subsequently processed off-line and the bispectrum evaluated.

A previous experiment [12] had shown that the dominant features in the spectrum, if stabilized by feedback such that the overall fluctuation level is diminished, does reduce transport. While a single feature observed in the spectrum is usually referred to as one mode, a question which arises is whether the plasma is in a turbulent state since many waves are required for turbulence and transport. We resolve the spectral width to reveal that the $\mathbf{E} \times \mathbf{B}$ mode is composed of radial harmonics. In Fig. 3 we track the amplitudes of individual frequencies across the plasma cross section, giving the radial structure of different individual frequency amplitudes. Frequencies with self-similar radial structures are grouped together to belong to the same radial harmonic. We observe two dominant self-similar structures, one from frequencies 73 to 75 kHz (labeled A) and another from 69 to 71 kHz (labeled B). The 72 kHz is most likely a combination of the other two. Radial harmonic A peaks at around 1.8 cm. Radial harmonic B, at the lower frequency band, has a bimodal structure with maxima at 1.2 and 2.4 cm. Clearly these radial harmonics contribute to the spectral width.

The existence of the radial harmonics along with their mode structures can be correlated with the bispectral analysis. The bispectral analysis was performed with a frequency resolution of 0.5 kHz ($\ll$ spectral width) to resolve these harmonics. Figure 4 shows the contour plot of the values of the autobicoherency (0.1–0.5) for a strong $\mathbf{E} \times \mathbf{B}$ mode for the three radial locations $r = 1.2$, 1.8, and 2.4 cm. The contour plot of the autobicoherency at the radius of 1.8 cm corresponding to the peak of radial harmonic A is shown in Fig. 4(b). It shows a strong coherent structure over the frequency range 73–75 kHz which identifies it as radial harmonic A. Moreover, additional coherent features at the lower frequency band appear at the radial locations 1.2 cm and 2.4 cm which correspond to the peaks for harmonic B and shown in the autobicoherency plots [Figs. 4(a) and 4(c)]. This leads us to conclude that the strong $\mathbf{E} \times \mathbf{B}$ mode in this case has two dominant radial harmonics.

The autobicoherency plot shown in Fig. 4(b) is replotted and shown in Fig. 5 with an expanded frequency range and with a lower cutoff of the autobicoherency values (0.05–0.5) to include the background turbulence. It shows that the coherent structure interacts with the turbulence as indicated by the trail of cross-coupling values corresponds to the frequency of ~ 72 kHz and the range 45–70 kHz. The spectral width at low fluctuation amplitudes can thus be linked to turbulent broadening.

The relationship between the coherence and the spectral width (FWHM) for both the $m = 1$, $\mathbf{E} \times \mathbf{B}$ mode and the $m = 2$ ITG mode are shown in Fig. 6. The bispectral analysis of the modes indicates that the auto-

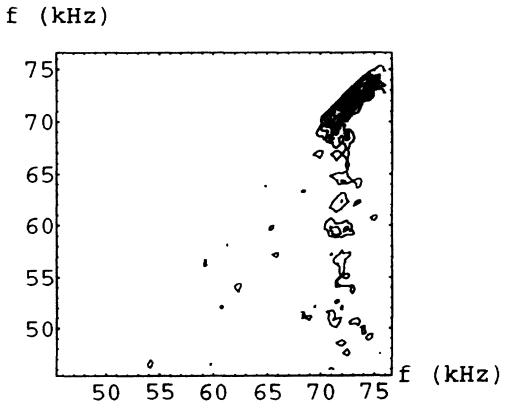

FIG. 5. Contour plot (0.05–0.5) at radius 1.8 cm showing interaction of coherence with turbulence.

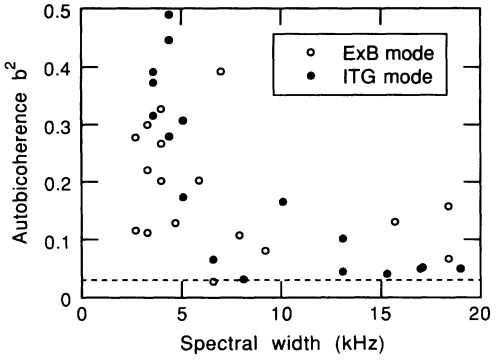

FIG. 6. Plot of autobicoherency values vs spectral width.

bicoherency values of both modes increase as the spectral width becomes narrower. Moreover, it shows clearly the two different coherence regimes with the narrower spectral width (< 5 kHz) corresponding to a highly coherent state ($b^2 \sim 0.2 - 0.5$) while the broader spectral width corresponds to turbulence or a low level of coherence ($b^2 \leq 0.1$). This affirms the conclusions drawn from Fig. 2. This would be consistent with a picture of a turbulent bath with a process of self-organization evolving into a quasicoherent state. Recently, Tsui *et al.* [10], using a Hasegawa-Mima type drift-wave turbulence equation, showed that the autobicoherency values could be related to the spectral width. In particular, they find that $\sum b^2(\omega_1, \omega_2) \approx 1 - (\nu_B/\omega)^2$, where ν_B is the turbulence frequency broadening. The trend in our result is consistent with their observation that the autobicoherency values increase as the spectral width decreases. This coherent state does not correspond, however, to the formation of solitons because they exhibit spectral broadening [8], which is inconsistent with our observation.

To summarize our results, we have experimentally obtained some simple scaling relationships between the electrostatic fluctuation levels and the linear growth rate. For the ion temperature gradient driven instability, a quadratic relationship was obtained, consistent with the quasilinear and weak turbulence limits. For the flute-like $\mathbf{E} \times \mathbf{B}$ mode, however, a linear scaling was obtained. This is indicative of the strong turbulence limit. Since turbulence and transport require the presence of many modes, the spectral width was resolved to identify radial harmonics. The coherent state of the $\mathbf{E} \times \mathbf{B}$ mode was composed of two radial harmonics. Moreover, for a high level of fluctuations, in the strong turbulence limit, the spectra became more coherent characterized by a narrowing of the spectral width. This result was explained by invoking the idea of self-organization. The observation of increased coherence was supported by a bispectral analysis. Both the turbulent and the coherent regimes exhibited linear scalings of fluctuation level with the linear growth rate. Such linear scalings are also consistent with the frequently used mixing length estimates for the strong turbulence case. This linear scaling, however, is in contrast to the quadratic scaling observed in previous experiments in the weak turbulence limit.

The authors acknowledge several fruitful discussions with Dr. Bin Song. This work was supported by the National Science Foundation Grant No. ECS-9004238.

[1] P.C. Liewer, Nucl. Fusion **25**, 543 (1985)
[2] W. Horton, Physics Reports, Nos. 1-3 (Elsevier Science Publishers, New York, 1990), Vol. 192, pp. 1–177.
[3] T.L. Rhodes, Ch. P. Ritz, and H. Lin, Phys. Rev. Lett. **65**, 583 (1990).
[4] T.H. Dupree, Phys. Fluids **9**, 1773 (1966).
[5] O. Ishihara, H. Xia, and A. Hirose, Phys. Fluids B **4**, 349 (1992).
[6] G.S. Lee and P.H. Diamond, Phys. Fluids **29**, 3291 (1986).
[7] M. Kono and E. Miyashita, Phys. Fluids **31**, 326 (1988).
[8] J.D. Meiss and W. Horton, Phys. Fluids **25**, 1839 (1982).
[9] U. Kauschke, Plasma Phys. Controlled Fusion **35**, 93 (1993).
[10] H.Y.W. Tsui, K. Rypdal, Ch. P. Ritz, and A.J. Wootton, Phys. Rev. Lett. **70**, 2565 (1993).
[11] R.G. Greaves, J. Chen, and A.K. Sen, Plasma Phys. Controlled Fusion **34**, 1253 (1992).
[12] A.B. Plaut, A.K. Sen, G.A. Navratil, and R. Scarmozzino, Phys. Fluids B **1**, 293 (1989).
[13] D.P. Dixon, A.K. Sen, and T.C. Marshall, Plasma Phys. **20**, 225 (1977).
[14] B.E. Keen and M.W. Alcock, Phys. Lett. **55A**, 25 (1975).
[15] B.B. Kadomtsev, *Plasma Turbulence* (Academic, London, 1965).
[16] P.W. Terry and W. Horton, Phys. Fluids **26**, 106 (1983).
[17] Y.C. Kim and E.J. Powers, IEEE Trans. Plasma Sci. **7**, 120 (1979).